JOURNAL OF MATERIALS SCIENCE 31 (1996) 1205–1211

# Formation of interface phases in the titanium alloy IMI 834

G. J. BAXTER, W. M. RAINFORTH
*Department of Engineering Materials, The University of Sheffield, Sheffield, S1 3JD, UK*
L. GRABOWSKI
*Rolls-Royce plc, PO Box 31, Derby, DE2 8BJ, UK.*

A variety of different preparation techniques have been used in order to identify the experimental conditions under which interface phases are formed in the near-α alloy, IMI 834. In particular, a Ni plated surface examined in cross-section in the TEM produced a gradation in hydrogen content from high at the surface to low levels in the bulk. Two transformation products have been identified, one was a monolithic f c c phase with a lattice parameter of $a = 0.434 \pm 0.004$ nm, which forms along α-platelet boundaries, and the second was an acicular feature which formed between α-platelet boundaries which was tentatively identified as an h c p phase twin related to the α-titanium. The monolithic interface phase was found to form at both low and high hydrogen levels while the α twins were only seen at high hydrogen contents. In all cases, the transformations were shown to be artefactual and induced solely by hydrogen absorption. No evidence of mechanical strain induced interface phase formation was found. In conflict with the literature, the monolithic f c c phase was found to occur during ion-beam milling and was attributed to water contamination of the milling gas. Formation of the interface phase was suppressed by electropolishing at temperatures $\leq -50\,^{\circ}C$.

## 1. Introduction

The detection of an interface phase (IFP) at the boundaries between the α-platelets (h c p) and retained-β (b c c) phases of various titanium alloys has, over the last two decades, been the subject of a wide variety of studies and considerable controversy [1–20]. In 1975, Rhodes and Williams [1] observed the interface phase by TEM as a distinct layer of between 0.1 and 0.4 μm wide in as many as 40 different titanium alloys. Two separate phases; a f c c monolithic phase and a striated phase, were commonly observed together [7–9] with the monolithic phase lying closer to the retained-β phase than the striated phase. The origins of these phases were clearly of importance as the α/β interface was believed to influence the fracture behaviour of titanium alloys, especially during fatigue and stress corrosion studies [3, 6]. An early study by Rhodes and Paton [7] suggested that a f c c monolithic phase and a h c p striated phase formed as intermediate transition phases during the β to α transformation. Subsequently, numerous investigators [4, 5, 8, 9–12] found the crystallography of the Rhodes–Paton model to be inapplicable to their alloys and an alternative origin for the IFP was proposed using electron diffraction studies, based on the similarities with the binary hydride of titanium, $TiH_2$. The monolithic phase was thought to form as a f c c, hydrogen induced phase which was stabilized by stress, strain or compositional gradients in the alloy [8, 9, 11]. The striated form of the IFP has generated more confusion and has been identified as either h c p [1, 2, 8, 13, 19] or f c c [7, 9–12, 14, 18] in structure.

It was later observed that the formation of the IFP was dependent on the thin foil preparation technique employed. The results obtained by various workers [13, 14, 17–19] suggested that the IFP's found in titanium alloys were thin foil artefacts which arise during the electropolishing process. The monolithic f c c phase was determined to be a hydride of titanium arising from an increase in hydrogen concentration and the striated phase was suggested to form as a result of stresses at the α/β interface arising from thin foil relaxation in the retained-β phase during electrolytic thinning [13, 17–19]. Thin foil preparation by ion-beam milling suppressed the retained-β phase relaxation [21] and was found to prevent the formation of both the monolithic and striated forms of the IFP [13, 14, 17, 19].

In the present study thin foils of the titanium alloy IMI 834 were prepared by electropolishing, ion-beam milling and a combination of both methods, to determine which preparation technique(s) induced the formation of the IFP in the alloy. In addition, an electrolytic nickel coating was applied which provided a gradation from very high hydrogen levels at the surface to low levels in the bulk.

0022–2461 

## 2. Experimental

IMI 834 is a commercial titanium alloy with near-α composition (wt %): 5.81 Al, 3.78 Sn, 3.39 Zr, 0.70 Nb, 0.45 Mo, 0.32 Si, 0.06 C, < 0.02 Fe, 885 p.p.m. 0 and 23 p.p.m. N. The alloy was solution treated at 1030 °C, oil quenched, aged for two hours at 700 °C and air cooled. In this condition the alloy has a duplex microstructure of equiaxed primary-α grains in a matrix of transformed-β grains containing colonies of similarly orientated α-platelets.

To provide a gradation of absorbed hydrogen, a polished surface was electroplated using a standard nickel Watts bath [22]. This surface was then examined in cross-section in the TEM using a technique adapted from those of Goodhew [23] and Newcombe *et al.* [24, 25]. This involved removing two specimens of size $2.0 \times 0.5 \times 10.0$ mm from the electroplated surface using a slow speed saw. Both electroplated surfaces were then brought together and glued using araldite into a slotted brass rod of 2 mm diameter. In this configuration the nickel plated surfaces were orientated along the rod diameter. The rod was subsequently glued into a brass tube of external diameter 3 mm. Discs were cut from the composite bar and carefully ground and polished to a thickness of 200 μm, followed by mechanical dimpling to 80 μm. The sample was then ion beam milled from both sides to electron transparency. Milling was carried out on a conventional stage of a Gatan Duomill operating at a voltage of 6 kV and a gun current of 0.5 mA. The angle of the beams was initially 16° to the surface and was reduced to 11° on perforation to improve the quality and extent of the electron transparent area. All thin foils were observed using a Jeol 200CX electron microscope operating at 200 kV.

In light of the results obtained from the nickel plated, cross-sectional foils, alternative preparation techniques were designed to determine the effects of the nickel plating, mechanical dimpling and ion beam milling stages of the foil preparation on the thin foil microstructure. 3 mm diameter discs of 0.5 mm in thickness were prepared from rods of IMI 834. The discs were ground on both sides using 1200 grit paper to a thickness of 200 μm. Foils were prepared by the following techniques: (i) electropolishing to perforation; (ii) dimpling to 80 μm remaining thickness and electropolishing to perforation; (iii) dimpling to 80 μm remaining thickness and ion-beam milled to perforation and (iv) electropolishing to 80 μm remaining thickness and ion-beam milled to perforation.

Electropolishing was carried out at 90 V and 0.22 A using a Struers Tenupol-2 electropolisher. A solution of 5% perchloric acid, 35% 2–butoxyethanol and 60% methanol, cooled with liquid nitrogen was used at a temperature of $\leq -50$ °C. All electropolished foils were cleaned twice in methanol before observation by TEM.

## 3. Results

Thin foils prepared by electropolishing showed no evidence of any interface phases along the α-platelet boundaries or across the width of the α-platelets. The microstructure, as shown in Fig. 1, comprised of α-platelets arranged in colonies within the transformed-β grains. The retained-β phase along the α-platelet boundaries in two adjacent colonies is shown in more detail in Fig. 2. The retained-β phase is present as an angular, discontinuous phase of 0.1 to 0.5 μm in width. This is clearly evident in the dark field micrograph, Fig. 2b, imaged using the $(0\,1\,1)_\beta$ reflection indicated. Although not in contrast in Fig. 2, dislocations arising from the lattice mismatch between the α-platelet and retained-β phases titanium–zirconium silicides of the

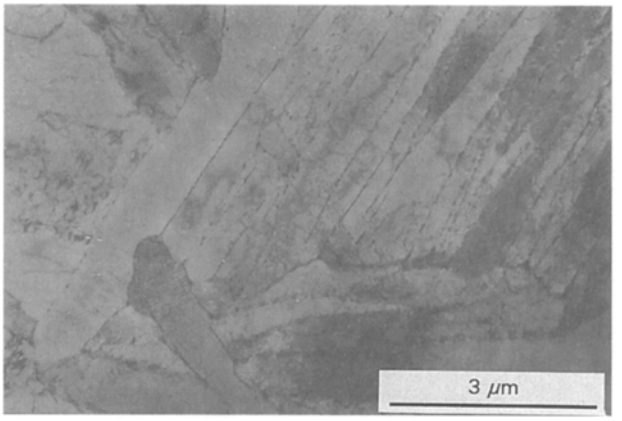


*Figure 1* Low magnification TEM micrograph showing the basket-weave α-platelets in the transformed-β grains.

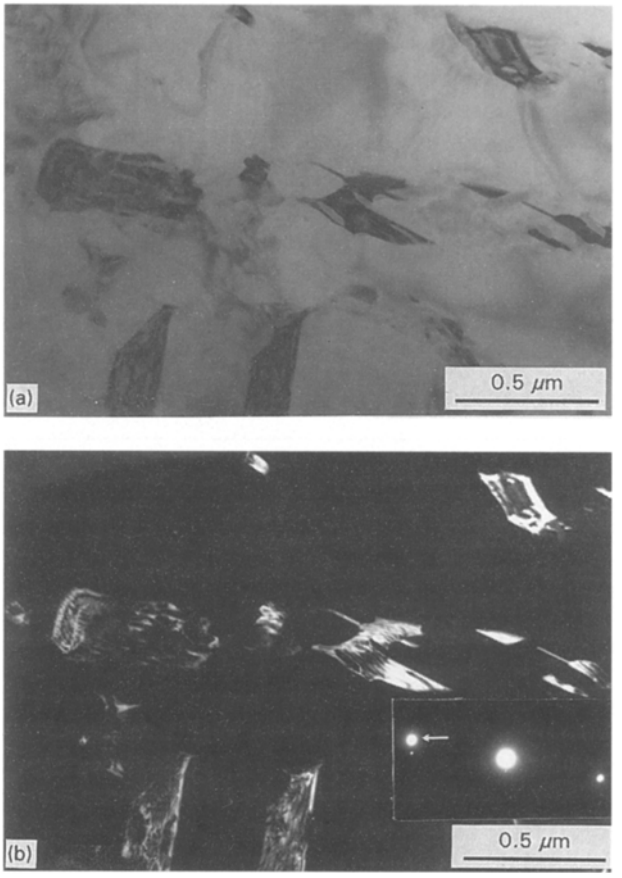


*Figure 2* (a) Bright field and (b) dark field micrographs showing the discontinuous retained-β phase along the α-platelet boundaries in a foil prepared by electropolishing. The corresponding β reflection is indicated in the accompanying diffraction pattern.

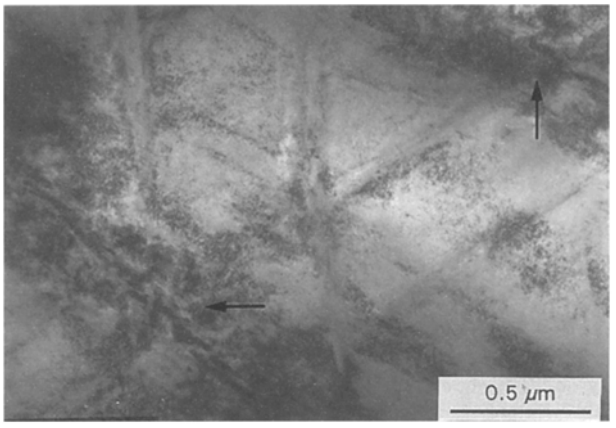


*Figure 3* TEM micrograph showing the appearance of the microstructure at approximately 100 μm from the plated surface. Two poorly defined α-platelet boundaries (indicated) are outlined on both sides by 0.3 μm wide bands of a third phase.

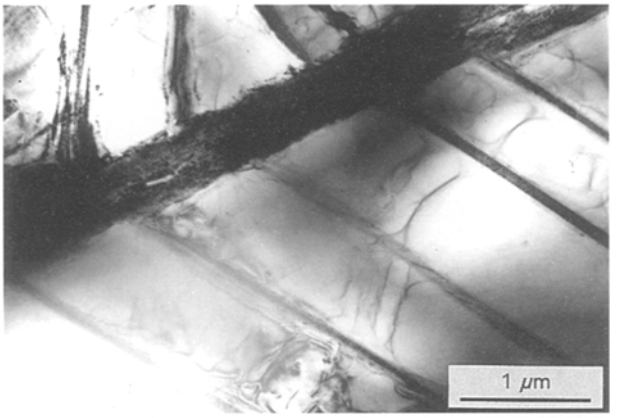


*Figure 4* Bright field TEM micrograph taken from approximately 150 μm from the plated surface. The features present in Fig. 3 are more clearly defined. A phase has formed along the α-platelet boundaries and acicular features of 0.02 to 0.2 μm wide have formed across the width of the α-platelets.

$S_2$ type ($a = 0.703 \pm 0.004$ nm, $c = 0.360 \pm 0.015$ nm) are present along the α-platelet boundaries.

The nickel plated sample exhibited a significant change in microstructure from the surface to the bulk. At approximately 100 μm from the surface in contact with the nickel plating the transformed-β microstructure was significantly different in comparison to that observed in electropolished foils. In Fig. 3, which is typical of the microstructure in this region, two α-platelet boundaries are present. The poorly defined boundaries are outlined on either side by bands of approximately 0.3 μm in width. Parallel streaks, which cross the α-platelets in several distinct directions between the α-platelet boundaries were also evident. The general microstructure was obscured by a high degree of residual strain in the foil sample.

Between approximately 150–250 μm from the plated surface the banding and streaking became more clearly defined, Figs 4 and 5a. The composite selected area diffraction pattern, Fig. 5b, was taken from the area imaged in Fig. 5a and is drawn schematically in Fig. 5c. The dark field micrographs, Fig. 5(d, e), were imaged using the reflections indicated in Fig. 5c. Two phases, which were distinct from the α and retained-β phases of titanium, had formed in the transformed-β microstructure. In Fig. 5d, a continuous phase of between 0.1 and 0.5 μm in width is shown to have formed along the boundaries between the α-platelets. Along the centre of the wider bands it is possible to distinguish thin films of the retained-β phase, as indicated in Fig. 5d. Acicular features of between 0.02 and 0.2 μm in width are highlighted in Fig. 5e which cross the width of the platelet-α in two crystallographic directions. In addition, this phase occurs along the interface between the boundary phase (Fig. 5d) and the α-platelet phase. On the evidence of over twenty measured diffraction patterns (including Figs 5b and 6a) and convergent beam diffraction patterns [22], the boundary phase was analysed as f c c in structure with a lattice parameter within the range $a = 0.434 \pm 0.004$ nm. The following orientation relationships were found between the α (h c p), β (b c c) and f c c crystal structures, and are illustrated in Figs 5(b, c) and 6(a, b):

$$[1\bar{2}13]_\alpha // [1\bar{1}2]_{fcc};\ (10\bar{1}0)_\alpha // (110)_{fcc} \quad (1)$$

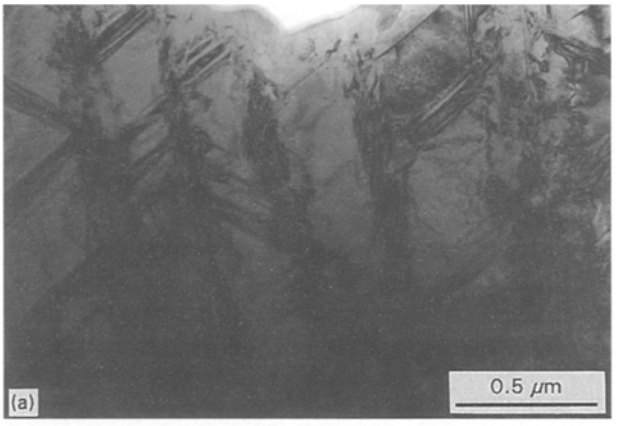


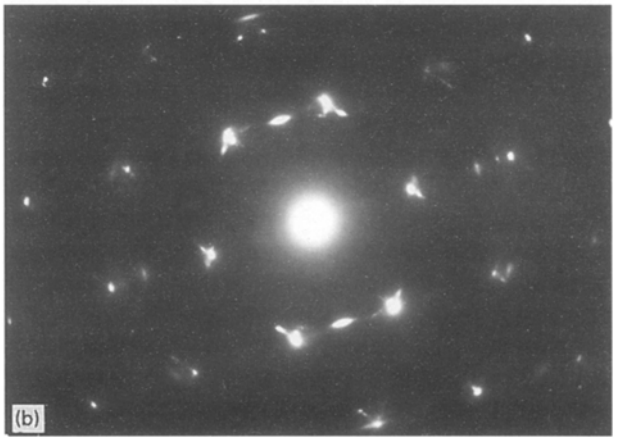


*Figure 5* (a) Bright field TEM micrograph of a region 150 μm from the plated surface of a cross-sectional thin foil showing the two features described in Fig. 4. (b) Composite selected area diffraction pattern containing reflections from both additional phases and reflections from a $[1\bar{2}13]_\alpha$ zone. (c) Schematic representation of (b) in which the reflections giving rise to each phase are distinguished. (d) Dark field micrograph taken of the same area as (a) using the reflection marked F to highlight the boundary phase. (e) Dark field micrograph taken of the same area as (a) using the reflection marked H to highlight the acicular phase across the α-platelets.

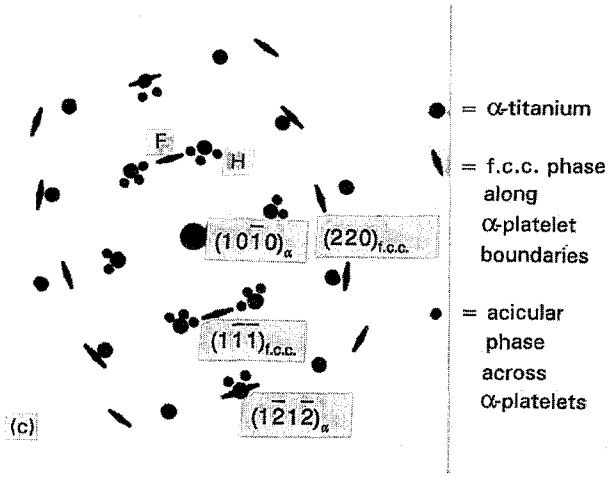


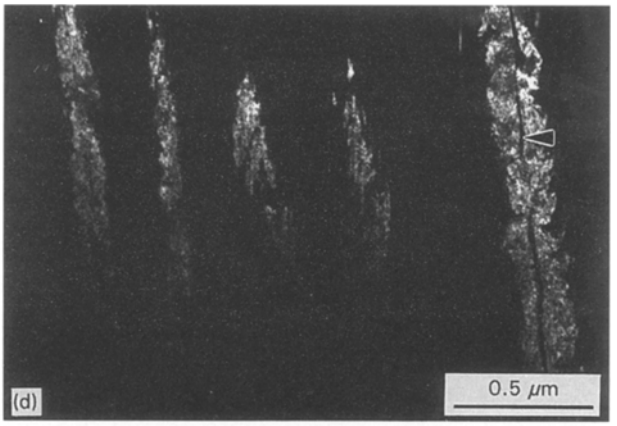


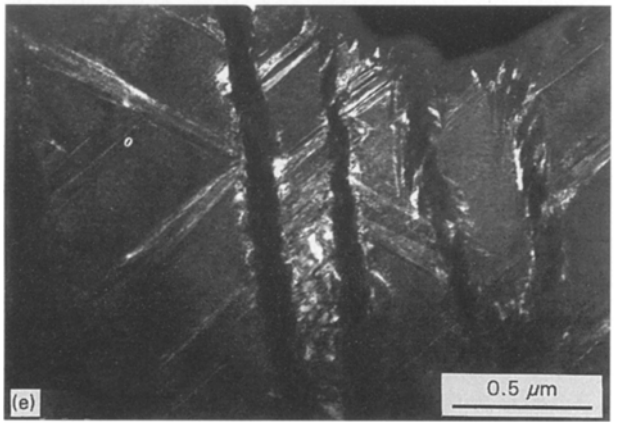


*Figure 5* (continued).

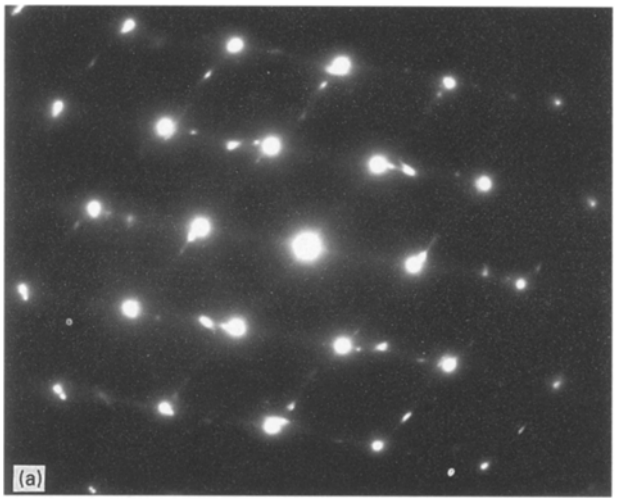


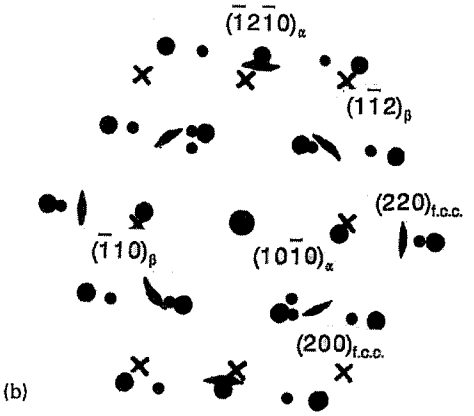


*Figure 6* (a) Composite selected area diffraction pattern taken from an area 150 μm away from the plated surface of a cross-sectional thin foil. The pattern contains reflections from α-titanium, the retained-β phase, a fcc phase along the α-platelet boundaries and an acicular phase across the α-platelets. (b) Schematic representation of (a) from which an orientation relationship between α-titanium, the retained-β phase and the fcc phase was determined.

$$[0\,1\,1]_\beta//[0\,0\,0\,1]_\alpha//[0\,0\,1]_{fcc};$$

$$(1\,\bar{1}\,2)_\beta//(1\,0\,\bar{1}\,0)_\alpha//(1\,1\,0)_{fcc} \quad (2)$$

The crystal structure of the acicular phase observed across the α-platelets (Figs 4 and 5e) could not be identified conclusively from the analysis of diffraction patterns. High resolution TEM of the phase also proved inconclusive since residual strain in the foil induced unacceptable distortions in the lattice fringe image. However, from the evidence obtained it appeared that the phase was most probably an hcp phase, which was $\{1\,0\,\bar{1}\,1\}$ twin related to the α-titanium, with a lattice parameter close to that of the α-titanium, as described by Banerjee *et al.* [13, 17, 19].

On moving further from the plated surface, the numbers of acicular bands observed across the α-platelets decreased, and none were observed at $> 250$ μm from the surface. However, the fcc boundary phase was observed along all the α-platelet boundaries in the electron transparent areas of the foil. No change in the structure of the primary-α phase was observed.

Some form of interface phase was found to form in all samples prepared by ion-beam milling. In order to verify that it was not the mechanical dimpling stage which strain induced the interface phase, samples were mechanically dimpled and then electropolished to perforation. As with the electropolished samples described earlier, no evidence of any additional phases either along the α-platelet boundaries or across the width of the α-platelets was found. IFP formation had therefore occurred during ion-beam milling. The fcc boundary phase had also formed in foils which were (i) electropolished and then ion-beam milled to perforation (Fig. 7) and (ii) dimpled and then ion-beam

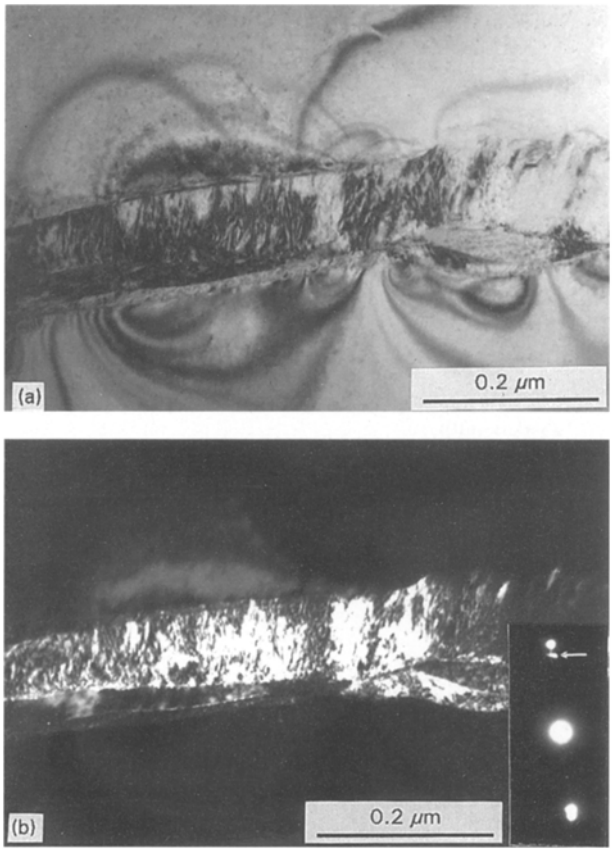


*Figure 7* (a) Bright field and (b) dark field TEM micrographs showing an example of the phase which was observed to occur along some of the α-platelet boundaries in a foil prepared by electropolishing and ion-beam milling. The reflection used to image (b) is indicated in the corresponding diffraction pattern.

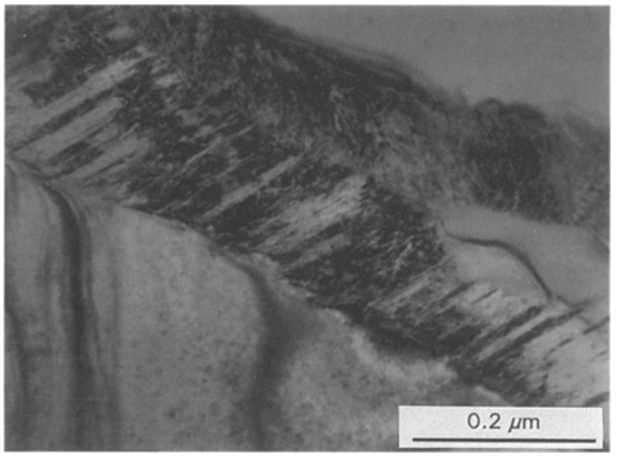


*Figure 8* Bright field TEM micrograph showing an example of the phase which was observed to occur along some of the α-platelet boundaries in a foil prepared by dimpling and ion-beam milling.

milled to perforation (Fig. 8). However, in these foils the phase had formed along only approximately half of the α-platelet boundaries and these were distributed randomly throughout the thin areas of the foils. No acicular features across the width of α-platelets were observed in foils prepared by either of these techniques.

## 4. Discussion

Table I summarises the results and compares the observations with those made in the literature. Table II provides a summary of the lattice parameters and orientation relationships for the IFPs reported in the literature.

The lattice parameter, $a = 0.434 \pm 0.004$ nm, determined for the fcc phase along the α-platelet boundaries lies within the range determined in the literature for the monolithic form of the IFP. The actual value of $a$ is dependent upon the alloy composition, prior heat treatment, cooling rate and/or foil preparation technique [5–13, 15, 17–20] and has been reported to lie between 0.420 nm [10] and 0.453 nm [19]. The two orientation relationships for the fcc phase found in the present investigation can simply be represented by the orientation relationship in Equation 2. This relationship agrees with that found by Hammond *et al.* [9, 16, 18] Banerjee *et al.* [19] for the monolithic fcc IFP. A different orientation relationship has been determined for a second crystallographic form of the fcc IFP which is referred to in the literature as the striated fcc IFP [10–13, 17–20]:

$$(1\bar{1}1)_{fcc}//(0002)_{\alpha}//(110)_{\beta};$$

$$[110]_{fcc}//[11\bar{2}0]_{\alpha}//[111]_{\beta} \quad (3)$$

It is concluded, therefore, that the fcc phase found in the present study is crystallographically identical to that observed in the literature for the monolithic fcc IFP.

The current results also confirm that the monolithic fcc IFP is a thin foil artefact which was formed during the ion-beam milling process and that no additional phases formed during electropolishing. The fact that the monolithic fcc IFP is a thin foil artefact is in agreement with the literature, however, the observations in the literature have found that this phase occurs as a result of an increase in hydrogen concentration during the electropolishing process [13, 17–19, 21]. This was clearly not the case in the current investigation where the formation of the IFP is suppressed by the use of electropolishing at very low temperatures. In addition, its presence could not be attributed to mechanical strain during thin foil preparation since it was not seen after mechanical grinding or dimpling. The IFP therefore appears to be solely related to the absorption of hydrogen, in agreement with Banerjee *et al.* [19].

The observation of an IFP after ion-beam milling is surprising since it is in conflict with the open literature and implies that there was a greater increase in hydrogen concentration in the foils during ion-beam milling compared to electropolishing. A possible explanation for this observation is that water may have been an impurity in the argon gas used during ion-beam milling. Hydrogen ions derived from this water may have been absorbed into the retained-β phase causing a volume expansion of the retained-β and thus causing the monolithic fcc IFP to form along some of the α-platelet boundaries.

In cross-sectional foils a hydrogen concentration gradient was established which was a maximum concentration at the surface and decreased as the distance into the bulk material increased. This provided a direct indication of the effect of hydrogen on the microstructure. At low hydrogen concentrations in regions

TABLE I A comparison of the effects of thin foil preparation techniques observed in the present investigation with those made in the literature

| Foil preparation technique | Effects observed in present study of IMI 834 | Effects observed in literature |
|---|---|---|
| Electropolished to perforation | No additional phases observed in any thin foils | Fcc interface phase observed as a thin foil artefact along the α-platelet boundaries and a hexagonal form of the interface phase observed across the α-platelet widths [13, 17–19, 21] |
| Foils prepared in cross-section by nickel plating, dimpling and ion-beam milling | A fcc phase of 0.1 to 0.5 μm present along all the α-platelet boundaries. A second phase also present across the α-platelet widths up to 250 μm away from the surface as acicular bands of 0.02 to 0.2 μm in width | ——— |
| Dimpled to 80 μm remaining thickness and electropolished to perforation | No additional phases observed in any thin foils | ——— |
| Dimpled to 80 μm remaining thickness and ion-beam milled to perforation | A fcc phase of 0.1 to 0.5 μm wide present along some the α-platelet boundaries | Ion-beam milling was found to prevent any interface phase formation [13, 17, 21] |
| Electropolished to 80 μm remaining thickness and ion-beam milled to perforation | A fcc phase of 0.1 to 0.5 μm wide present along some of the α-platelet boundaries | ——— |

TABLE II Lattice parameters and orientation relationships suggested for the interface phases

| Reference | $a$ (nm) | Phase | Orientation relationship |
|---|---|---|---|
| 5 | 0.433 | M | $(0001)_\alpha // (001)_{fcc}$; $\langle 11\bar{2}0\rangle_\alpha // \langle 110\rangle_{fcc}$ |
| 6 | 0.426 | M | $(0001)_\alpha // (110)_{fcc}$; $[11\bar{2}0]_\alpha // [111]_{fcc}$ |
| 7 | 0.426 | M | $(0002)_\alpha // (111)_{fcc} // (110)_\beta$; $[11\bar{2}0]_\alpha / [\bar{1}10]_{fcc} // [\bar{1}11]_\beta$ |
| 8 | 0.436 | M | $(0001)_\alpha // (111)_{fcc} // (110)_\beta$; $\langle 11\bar{2}0\rangle_\alpha / \langle 110\rangle_{fcc} // \langle 111\rangle_\beta$ |
| | | S, hcp | $(10\bar{1}0)_\alpha // (10\bar{1}0)_p$; $\langle 0001\rangle_\alpha // \langle 1\bar{2}13\rangle_p$ |
| 9 | 0.435 | M | $(0002)_\alpha // [110]_\beta // [001]_{fcc}$; $(1\bar{2}10)_\alpha // (1\bar{1}\bar{1})_\beta // (\bar{1}10)_{fcc}$ |
| | | S | One variant obeyed the above relationship |
| 11, 12 | 0.44 | M | $(1\bar{1}0)_{fcc} // (1\bar{1}00)_\alpha$; $[001]_{fcc} // [0001]_\alpha$ |
| | | S | $(111)_{fcc} // (0001)_\alpha$; $[1\bar{1}0]_{fcc} // [11\bar{2}0]_\alpha$ |
| 13 | — | M | $(001)_{fcc} // (0001)_\alpha$; $[110]_{fcc} // [11\bar{2}0]_\alpha$ |
| | | S | $(111)_{fcc} // (0001)_\alpha$; $[110]_{fcc} // [11\bar{2}0]_\alpha$ |
| | | hcp | $\{10\bar{1}1\}$ twin related to the α phase |
| 15 | 0.434 | S | |
| 17 | | M | $(110)_{fcc} // (1\bar{1}00)_\alpha$; $[001]_{fcc} // [0001]_\alpha$ |
| | | S | $(111)_{fcc} // (0001)_\alpha$; $[1\bar{1}0]_{fcc} // [11\bar{2}0]_\alpha$ |
| | | hcp | $\{10\bar{1}1\}$ twin related to the α phase |
| 10, 18 | 0.420, 0.425 | S | $\{111\}_{fcc} // (0001)_\alpha // \{110\}_\beta$; $\langle 110\rangle_{fcc} // \langle 1\bar{2}10\rangle_\alpha // \langle 111\rangle_\beta$ |
| | | S | $\{001\}_{fcc} // (0001)_\alpha // \{110\}_\beta$; $\langle 110\rangle_{fcc} // \langle 11\bar{2}0\rangle_\alpha // \langle 111\rangle_\beta$ |
| 19 | 0.453 | M | $(1\bar{1}0)_{fcc} // (1\bar{1}00)_\alpha // (1\bar{1}2)_\beta$; $[001]_{fcc} // [0001]_\alpha // [110]_\beta$ $[110]_{fcc} // [11\bar{2}0]_\alpha // [1\bar{1}\bar{1}]_\beta$ |
| | | S | $(111)_{fcc} // (0002)_\alpha // (110)_\beta$; $[1\bar{1}0]_{fcc} // [11\bar{2}0]_\alpha // [1\bar{1}1]_\beta$ |

M = monolithic phase
S = striated phase

well below the nickel plated surface (Fig. 9), the monolithic interface phase was the only hydrogen induced phase observed (Figs 4, 5). No difference in lattice parameter was found for this phase at different depths below the nickel plated surface and in other samples produced by ion milling. This indicates, as expected, that the lattice parameter of this phase is dictated by the alloy composition and not the hydrogen content.

On observing the transformed-β microstructure closer to the nickel-plated surface an increase in hydrogen content led to an increase in the monolithic fcc IFP thickness and then to the formation of an additional transformation product. Unfortunately, a conclusive identification of the acicular features could not be determined in the present work. However, from the evidence available, they appeared to be the hcp phase,

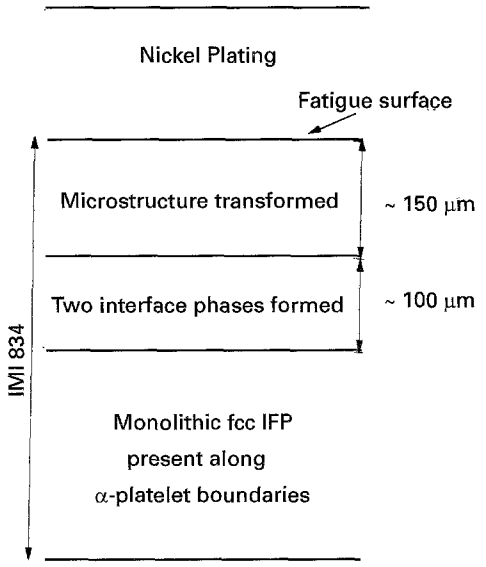


*Figure 9* Schematic diagram summarizing the effects caused by the nickel plating process on the thin foil microstructure of cross-sectional foils of IMI 834.

$\{1\,0\,\bar{1}\,1\}$ twin related to the α-titanium and with lattice parameters similar to the α-titanium. It is suggested that these twins were caused when the concentration of hydrogen had reached a level whereby the stresses imposed by the expansion of the retained-β phase could not be accommodated by the monolithic fcc IFP formation alone. The current observations agree with those in the literature [8, 13, 17, 19]. For example, Banerjee *et al.* [19] found an hcp phase in electropolished foils of Ti–10V–2Fe–3Al, with six variants formed by twinning on the six possible $\{1\,0\,\bar{1}\,1\}$ planes of the parent α-platelets. The hcp phase was believed to be formed by the volume expansion of the retained-β phase and concomitant compression of the phase due to hydrogen absorption during electropolishing.

## 5. Conclusions

1. No evidence of any interface phases was found in foils of the titanium alloy IMI 834 which were prepared by electropolishing.
2. The monolithic form of the fcc interface phase ($a = 0.434 \pm 0.004$ nm) was identified to form along some of the α-platelet boundaries in thin foils prepared by techniques involving an ion-beam milling stage. This is in conflict with the literature.
3. It is proposed that water may have been an impurity in the argon gas used during ion-beam milling and that hydrogen ions derived from this water may have led to the formation of the fcc interface phase.
4. From the observations of cross-sectional thin foils, it is concluded that the nickel plating process used in their preparation had caused hydrogen absorption into the bulk titanium. As the hydrogen concentration increased (i) the monolithic fcc IFP formed along the α-platelet boundaries, (ii) an acicular phase of approximately 0.1 μm in width occurred across the width of α-platelets and (iii) at high hydrogen concentrations, the entire transformed-β microstructure was altered.
5. The results add to the evidence that the IFP's are artefacts induced by thin foil preparation.

## References

1. C. G. RHODES and J. C. WILLIAMS, *Metall. Trans. A.* **6A** (1975) 1670.
2. H. MARGOLIN, E. LEVINE and M. YOUNG, *ibid.* **8A** (1977) 373.
3. I. W. HALL and C. HAMMOND, *Mater. Sci. Eng.* **32** (1978) 241.
4. I. W. HALL, *Scand. J. Metals* **7** (1978) 277.
5. *Idem, Metall. Trans. A.* **9A** (1978) 815.
6. I. W. HALL and C. HAMMOND, *Metal Sci.* **12** (1978) 339.
7. C. G. RHODES and N. E. PATON, *Metall. Trans. A.* **10A** (1979) 209.
8. I. W. HALL, *Scand J. Metals* **8** (1979) 17.
9. P. HALLAM and C. HAMMOND, in "Titanium '80, Science and Technology", edited by H. Kimura and O. Izumi, (TMS-AIME, Warrendale, PA, 1980) vol. 2, p. 1435.
10. G. C. MORGAN and C. HAMMOND, *ibid.* vol. 2. p. 1443.
11. D. BANERJEE and V. S. ARUNACHALAM, *Acta metall.* **29** (1981) 1685.
12. D. BANERJEE, *Metall. Trans. A.* **13A** (1982) 681.
13. D. BANERJEE and J. C. WILLIAMS, *Scripta metall.* **17** (1983) 1125.
14. C. G. SHELTON and B. RALPH, in "Proc. Conf. The Metallurgy of Light Alloys", (I.S.O.M. Conf. No. 20, 1983) p. 180.
15. N. R. MOODY, F. A. GREULICH and S. L. ROBINSON, *Metall. Trans. A.* **15A** (1984) 1955.
16. C. HAMMOND, R. A. SPURLING and N. E. PATON, *ibid.* **15A** (1984) 813.
17. D. BANERJEE, C. G. RHODES and J. C. WILLIAMS, in "Titanium Science and Technology", edited by G. Lütjering, U. Zwicker and W. Bunk, (DGM, Oberursel, Germany, 1985) vol. 3, p. 1597.
18. G. H. ISAAC and C. HAMMOND, in *ibid* vol. 3, p. 1605.
19. D. BANERJEE, C. G. SHELTON, B. RALPH and J. C. WILLIAMS, *Acta metall.* **36** (1988) 125.
20. C. SERVANT, C. QUESNE, T. BAUDIN and R. PENELLE, *J. Mater. Res.* **6** (1991) 987.
21. R. A. SPURLING, C. G. RHODES and J. C. WILLIAMS, *Metall. Trans. A.* **5** (1974) 2597.
22. G. J. BAXTER, Ph.D. Thesis, Sheffield University, Sheffield 1994.
23. P. J. GOODHEW, "Thin Foil Preparation for Electron Microscopy" (Elsevier, Oxford, UK, 1985) p. 139.
24. S. B. NEWCOMB, W. M. STOBBS and C. B. BOOTHROYD, *J. Microscopy* **140** (1985) 195.
25. S. B. NEWCOMB, C. S. BAXTER and E. G. BITHELL, *Inst. Phys. Conf. Ser.* **93** (1988).

*Received 21 March 1995*
*and accepted 8 September 1995*